Journal of Non-Crystalline Solids 463 (2017) 158–162

Contents lists available at ScienceDirect

Journal of Non-Crystalline Solids

journal homepage: www.elsevier.com/locate/jnoncrysol

Structural and optical study of glasses in the TeO_2-GeO_2-PbF_2 ternary system

Camila Pereira [a], Fabia C. Cassanjes [a], Juliana S. Barbosa [a], Rogeria R. Gonçalves [b], Sidney J.L. Ribeiro [c], Gael Poirier [a,*]

[a] Grupo de Química de Materiais, Universidade Federal de Alfenas, Campus de Poços de Caldas, Poços de Caldas, MG, Brazil
[b] Departamento de Química, Faculdade de Filosofia, Ciências e Letras de Ribeirão Preto, Universidade de São Paulo, Av. Bandeirantes, 3900, 14040-901, Ribeirão Preto, SP, Brazil
[c] Instituto de Química, Universidade Estadual Paulista Júlio de Mesquita Filho, Araraquara, SP, Brazil

ARTICLE INFO

Article history:
Received 4 December 2016
Received in revised form 22 February 2017
Accepted 26 February 2017
Available online 11 March 2017

Keywords:
Glass
Tellurite
Fluoride
Photoluminescence

ABSTRACT

New glass compositions were investigated in this specific proportion (90-x)TeO_2-10GeO_2-xPbF_2 in order to study the influence of lead fluoride content on the thermal, structural and optical properties. Glass samples with x = 5 to 30% were prepared by melt-quenching method. Thermal characterizations by DSC allowed to identify a clear decrease of the glass transition temperature as well as a very distinct crystallization behavior for higher PbF_2 contents. Raman spectroscopy suggests a progressive PbF_2 incorporation with conversion of TeO_4 to TeO_3 units related with the modifier behavior of PbF_2 in the glass network. X-ray diffraction patterns of crystallized samples support these results since crystalline TeO_2 was detected for lower PbF_2 contents whereas lead tellurite $Pb_2Te_3O_7$ was identified for the most lead fluoride concentrated sample. UV–Vis–NIR absorption spectra are in agreement with a progressive increase of the optical bandgap with lead fluoride concentration. Emission spectra of Eu^{3+} doped samples also pointed out a progressive structural change around Eu^{3+} ions with more symmetric sites. Finally, experimental lifetimes, Judd-Ofelt parameters and quantum efficiencies were obtained from these samples and exhibited a strong dependency of the lead fluoride contents, suggesting that these new fluorotellurite glasses are interesting hosts for rare earth ions.

1. Introduction

TeO_2 based glasses were intensively studied since their discovery in 1950s [1]. In fact, tellurite glasses combine unique properties among oxide glasses such as low phonon energy, high infrared transmittance, high linear and non-linear optical indices, low melting temperatures and good chemical stabilities [2,3]. These properties are related with local order around tellurium atoms, explaining why structural evolution with composition has been investigated by several authors by means of X-ray diffraction and Raman spectroscopy [2,4].

On the other hand, heavy metal fluoride glasses have attracted considerable interest for optical applications since several properties such as infrared transmission and low phonon energy cannot be reached in oxide glasses. Particularly, fluoride glasses are very efficient hosts for luminescent ions since non radiative relaxations are minimized in this chemical environment [5]. However, these materials often present low chemical and thermal stability, which make their manufacturing more complicated and more expensive. For these reasons, oxyfluoride glasses and glass-ceramics are key materials since they combine the superior optical properties of fluoride materials together with the higher chemical and thermal stability of oxide glasses.

GeO_2 addition is a well known glass former and is often used in glass science in order to stabilize glass compositions with low thermal stability against devitrification and can be helpful to enhance the thermal and chemical properties of glasses in the binary system TeO_2-PbF_2 [6]. Despite the slight increase of phonon energy with GeO_2 addition, the gain in thermal properties opens opportunities for rare earth doping of these compositions with final interesting optical properties [7–12].

Based on these considerations, vitreous compositions were investigated in the ternary system TeO_2-GeO_2-PbF_2 in order to identify stable compositions with high lead fluoride contents. The thermal and structural properties were investigated in function of the PbF_2 content by thermal analysis, X-ray diffraction of the crystallized samples and Raman spectroscopy. Optical properties were also studied using UV–Vis absorption and Eu^{3+} photoluminescence which allowed to determine experimental lifetimes and quantum efficiency versus composition.

2. Experimental part

Ternary glass samples were prepared by traditional melt-quenching for molar specific proportion (90-x)TeO_2-10GeO_2-xPbF_2 with *x* varying from 5 to 30. Firstly, powdered precursors such as tellurium oxide, TeO_2

* Corresponding author at: Instituto de Ciência e Tecnologia, Campus de Poços de Caldas – UNIFAL-MG, Rodovia José Aurélio Vilela 11999, Cidade Universitária, Poços de Caldas, MG CEP 37715-400, Brazil.
E-mail address: gael.poirier@unifal-mg.edu.br (G. Poirier).

http://dx.doi.org/10.1016/j.jnoncrysol.2017.02.021
0022-3093/

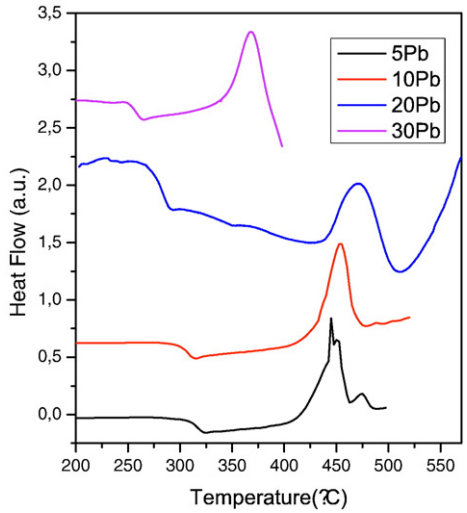

Fig. 1. DSC curves of glass samples.

(99 +%, Aldrich), germanium oxide, GeO_2 (99.9%, Aldrich) and lead fluoride PbF_2 (99.9% Aldrich) were mixed and melted in a covered gold crucible at 800 °C for 10 min. The melt was cooled in a brass mold at room temperature resulting in transparent glasses samples. Two sets of glass samples were prepared: the first labeled xPb from undoped ternary glasses and the second labeled xPbEu for Eu^{3+} doped samples.

Thermal properties were investigated using a DSC calorimeter F3 Maia from *Netzch*, 15 mg of bulk samples were heated in an Al hermetic pan (10 K/min and 50 mL·min^{-1} of N_2 flux) in the range of 150–600 °C. Crystallized samples were analyzed by X-ray diffraction with a Rigaku Ultima IV diffractometer using Cu Kα radiation, 2θ investigation was in 3–70° range with a step pass of 0.02° and a step time of 1 s. Raman spectra of bulk glass samples were obtained using a Jobin-Yvon Horiba-HR800, working with a He/Ne-laser at 632.8 nm. UV–visible spectra were recorded using Cary 7000 spectrophotometer from 200 to 2000 nm. Refractive index was obtained with Metricon M-Lines equipment under 534 nm laser. Europium photoluminescence measurements were obtained using a Horiba Jobin Yvon Fluorolog spectrofluorometer. Eu^{3+} doped samples were excited using a Xe continuous lamp of 450 W, thus obtaining the excitation and emission spectra. The experimental conditions were slit excitation of 3 nm, slit emission of 2 nm with a step of 0.5 nm and acquisition time of 0.2 s. Lifetimes measurement was obtained from Xe pulsed lamp excitation with 4 nm for excitation and emission slits and 0.05 nm for delay increment.

3. Results and discussion

Transparent and homogeneous glass samples were obtained in the specific proportion (90-x)TeO_2-10GeO_2-xPbF_2 for PbF_2 content x ranging from 5 to 30%. Since oxyfluoride tellurite glasses are hardly obtained in the binary system TeO_2-PbF_2 because of their high crystallization tendency on cooling, germanium oxide has been incorporated in a constant proportion of 10% in order to stabilize these compositions. The glassy state has been verified by the presence of a glass transition temperature and lack of diffraction peaks in the X-ray diffraction pattern. For higher concentrations, the melt spontaneously crystallized, at least partially, during quenching. DSC curves for undoped bulk glass samples are presented in Fig. 1. Characteristic temperatures extracted from DSC curves, thermal stability parameters: Tx − Tg, H = (Tx − Tg) / Tg, S = (Tx − Tg) / (Tp − Tx) / Tg used to determine the glass stability versus crystallization and visual aspect of undoped samples xPb are listed in Table 1. Tg temperatures decreased with PbF_2 addition together with thermal stability parameters. From a general first approach, this Tg decrease is a clear indication that lead fluoride is being incorporated inside the tellurium germanium oxide vitreous network. Fluoride compounds are well-known glass modifiers in oxide networks with formation of terminal metal-fluorine bonds. This behavior may be related to a very important parameter in the glass chemistry which is glass network connectivity. High Tg values indicate greater connectivity, so according to composition it was found that samples with higher TeO_2

Table 1
Composition, thermal properties and visual aspect of xPb samples.

Samples	Tg/°C	Tx/°C	Tc_1/°C	Tc_2/°C	Tx-Tg/°C	H	S	Picture
5Pb	310	410	445	473	100	0.32	11.29	
10Pb	300	420	452	–	120	0.40	12.80	
20Pb	275	411	466	–	136	0.49	27.2	
30Pb	250	313	374	–	63	0.25	15.37	

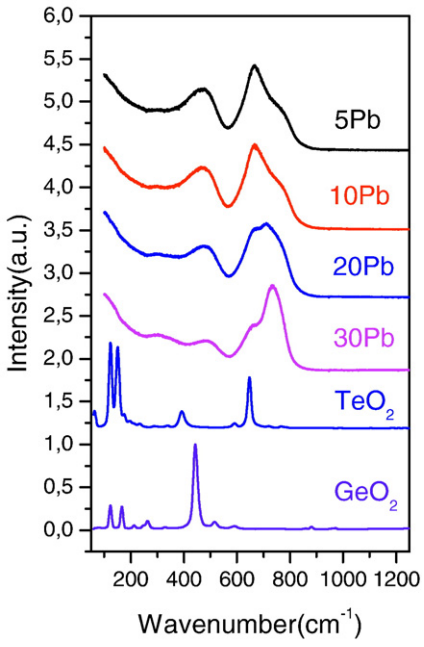

Fig. 2. Raman spectra of glass samples and crystalline reference GeO_2 and TeO_2.

concentration exhibit higher connectivity whereas PbF_2 addition decreases this overall connectivity. For our samples this behavior was expected because it can be assumed that lead fluoride promotes a progressive break of Te—O—Te and Te—O—Ge bridging bonds and formation of terminal Te—F and Ge—F bonds. Together with Tg, thermal stability parameters for this samples varied in the same way, as seen in Table 1. PbF_2 addition induces a higher tendency for devitrification under heating, suggesting again a lower viscosity above Tg related with a less connected network.

Structural evolution versus composition was largely investigated in tellurite glasses by Raman measurements, X-ray absorption spectroscopies and Te NMR [13–15]. These techniques reveal that Te atoms are able to form three distinct polyhedra with O atoms depending on the composition and modifier content. For glasses with highest TeO_2 amounts, the main unit is trigonal bipyramids represented by TeO_4. Upon modifier addition occurs a conversion to TeO_{3+1} unit, where $Te–O_{ax}$ distance is elongated. When the modifier content reaches a higher level, TeO_3 units are dominant [16–19]. TeO_4 units promote higher connectivity of the glass network, whereas trigonal pyramids TeO_3 result in a less connected glass. Raman spectra, presented in Fig. 2, clear pointed out structural changes with composition. Raman bands were analyzed in three wavenumber regions. The first and second around 485 cm^{-1} and 675 cm^{-1}, respectively, intensity of Raman bands decreases in intensity with PbF_2 contents. The third near 750 cm^{-1} increases with PbF_2 addition. Fig. 3 presents the deconvolution of bands between 570 and 850 cm^{-1}, providing important information about structural evolution in this system, regarding the shape and area evolution of the considered Raman bands. In Fig. 3, Raman band labeled 1 is attributed to TeO_4 units, band 2 due to TeO_{3+1} and band 3 associated with TeO_3 units. Lead fluoride insertion in the TeO_2—GeO_2 network causes an elongation of Te—O_{ax} bonds in TeO_4 units leading to the formation of TeO_{3+1} and alsoTeO_3 units for the most PbF_2 concentrated samples. In fact, Raman bands intensities between 460 cm^{-1} and 650 cm^{-1} related with stretchings in TeO_4 units gradually decrease with x increase whereas another band at 760 cm^{-1} associated to TeO_3 units increases in intensity. This observation is in agreement with a progressive incorporation of PbF_2 inside the tellurite germanate glass network leading to a progressive conversion of TeO_4 to TeO_3 [20]. It must be noted that the modifier behavior of PbF_2 can be understood considering the formation of Te—F terminal bonds, suggesting that part of the Te—O bonds in TeO_4 and TeO_3 units might be replaced by Te—F bonds even if these tellurium fluorine linkages were not clearly identified by Raman spectroscopy. This structural evolution is also supported by X-ray diffraction data obtained from glass samples that were crystallized by heat treatment at the crystallization temperature obtained from DSC curves as shown in Fig. 4. In fact, crystallized samples with higher TeO_2 contents exhibited the preferential formation of paratellurite α TeO_2 (11–693 in Inorganic Crystal Structure

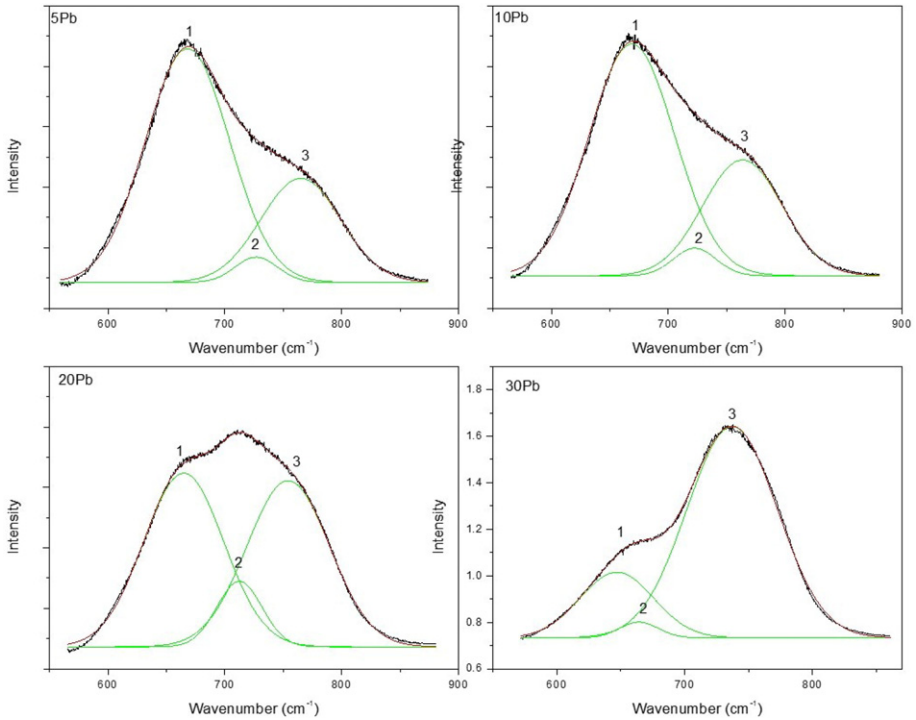

Fig. 3. Deconvolution of Raman bands for glass samples.

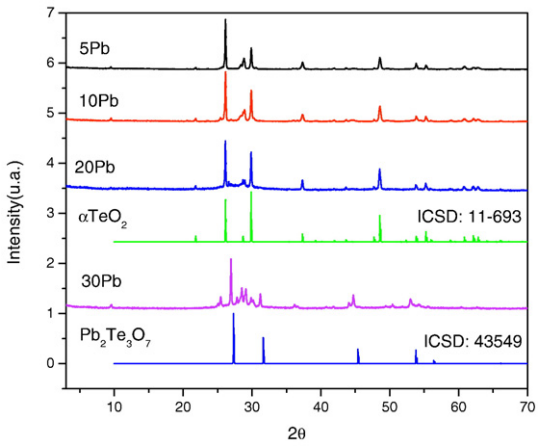

Fig. 4. X-ray diffraction patterns of crystallized samples after heat-treatment at the first crystallization temperature.

Database) constituted of trigonal bypiramids TeO_4 whereas the sample 30Pb exhibited diffraction peaks in agreement with the presence of lead tellurite $Pb_2Te_3O_7$ built from TeO_3 trigonal pyramids (43,549 in Inorganic Crystal Structure Database). Such crystallization behavior strongly suggests that these tellurium oxide units are dominant proportion in the respective starting glasses.

UV–Vis–NIR absorption spectra of the prepared glasses are presented in Fig. 5 between 300 and 2500 nm and the spectra were used to determine the energy bandgap in function of composition resumed in Table 2 together with their refractive index. PbF_2 addition promote an increase of the optical bandgap which can be related with a higher ionic character of the glass network since covalently bonded elements are substituted by highly ionic ones such as Pb^{2+} and F^-. On the other hand, the most PbF_2 concentrated sample 30Pb does not follow this behavior since the bandgap energy is close to glass 5Pb. Such behavior is not expected based on the previous structural assumptions built from thermal analysis and Raman results but can be tentatively related with the formation of defects and color centers for this composition. The overall decrease of refractive index values is in agreement with a decrease of the glass network polarizability. These results support the assumption of an effective insertion of lead fluoride in the glass network.

In order to investigate the influence of glass composition on rare earth luminescent properties and further access additional structural information, these glass compositions were doped with Eu^{3+} used as a structural probe. Emission spectra of the samples under 393 nm

Table 2
Ratio of intensity between the transitions $^5D_0 \rightarrow {}^7F_2$ and $^5D_0 \rightarrow {}^7F_1$, band gap energy and refractive index for xPb samples.

Samples	$^5D_0 \rightarrow {}^7F_2/{}^5D_0 \rightarrow {}^7F_1$	Band gap (eV)	Refractive index
5PbEu	3.16	3.27	2.1394
10PbEu	2.94	3.34	2.1238
20PbEu	2.70	3.43	2.1196
30PbEu	2.08	3.28	2.1076

excitation are presented in Fig. 6, in which all spectra were normalized at the maximum emission band related with electronic transition $^5D_0 \rightarrow {}^7F_1$. Emission bands were observed at 577 nm related with $^5D_0 \rightarrow {}^7F_0$ transition, 591 nm from $^5D_0 \rightarrow {}^7F_1$, 612 nm from $^5D_0 \rightarrow {}^7F_2$ and 703 nm from $^5D_0 \rightarrow {}^7F_4$. It is well-known that this electronic transition is magnetic dipole transition and is not affected by the ligand field around Eu^{3+} whereas electronic transition $^5D_0 \rightarrow {}^7F_2$ is an electric dipole transition and its intensity is strongly dependent of the atomic environment. Thus, the intensity ratio between these two emission bands provides an estimate of the symmetry degree around Eu^{3+} ion. Values less than 1 or near 0 are indicative of highly symmetric sites whereas values near 10 are typically related with low symmetry sites as often observed in glasses. Intensity of radiative transition $^5D_0 \rightarrow {}^7F_0$ also depends on the symmetry of Eu^{3+} site and is forbidden to centrosymmetric sites [21]. Intensity ratio between the emission bands due to $^5D_0 \rightarrow {}^7F_2$ and $^5D_0 \rightarrow {}^7F_1$ is dependent of the glass compositions as seen in Fig. 6 and the values presented in Table 2 varied from 3.16 for sample Pb5Eu to 2.08 for sample Pb30Eu. This decrease is a strong suggestion of a chemical and geometrical change in the Eu^{3+} environment related with a partial substitution of oxygen atoms by fluorine atoms and a resulting more symmetric first coordination shell. This model is further supported by the experimental lifetimes and quantum efficiencies resumed in Table 3. Radiative lifetimes of electronic level $^5D_0$ slightly increase from 0.84 ms to 1.27 ms with increasing the PbF_2 content, pointing out that radiative electronic relaxations are favored in sample Pb30Eu when compared to the less PbF_2 concentrated samples. This behavior is in agreement with a progressive decrease of the local phonon energy around Eu^{3+} due to a richer fluorine neighborhood. Quantum efficiencies were obtained from the emission band areas using the Judd-Ofelt theory in order to access the Judd-Ofelt parameters Ω_2 and Ω_4 and calculate the radiative theoretical lifetime τ_{rad} [23]. Quantum efficiencies are then obtained from the ratio between experimental and radiative lifetimes. Ω_2 is related with the covalent character of local network bonds around Ln^{3+}, high Ω_2 values indicating high covalence and low

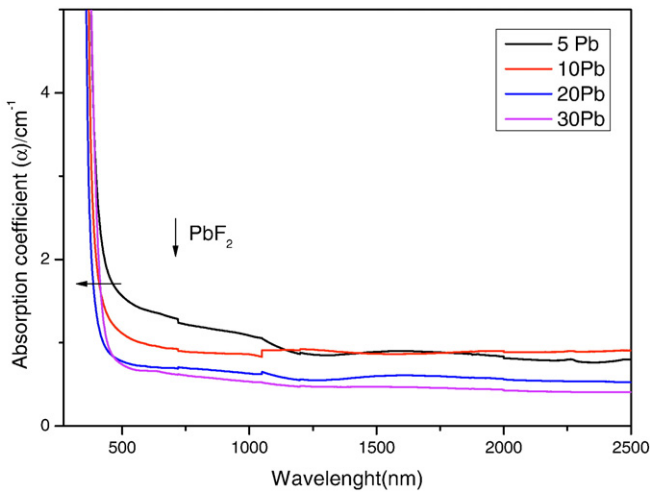

Fig. 5. UV–Visible-NIR absorption spectra of glass samples.

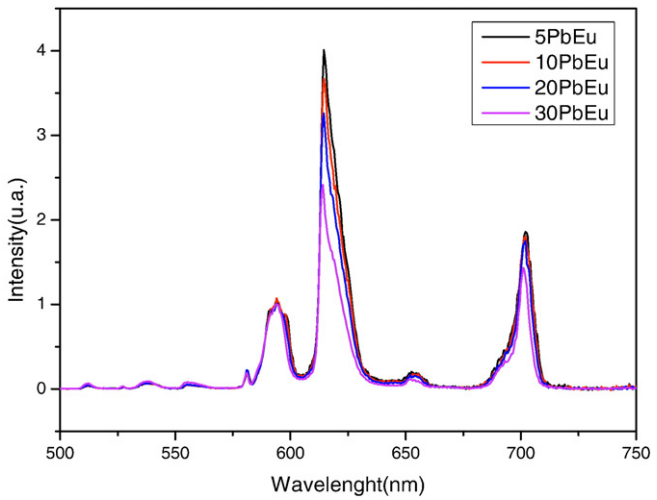

Fig. 6. Eu^{3+} emission spectra of glass samples under 393 nm excitation.

Table 3
Lifetimes and quantum efficiency for xPb samples.

Samples	$^5D_0$ lifetime (ms) Excitation at 393 nm	Ω_2 (10^{-20} cm^2)	Ω_4 (10^{-20} cm^2)	τ_{rad} (ms)	Quantum efficiency (%)
5PbEu	0.84	4.75	3.75	1.23	68.25
10PbEu	0.90	4.41	3.57	1.33	67.63
20PbEu	0.98	4.14	3.36	1.42	69.07
30PbEu	1.27	3.25	2.69	1.75	72.49

symmetry whereas Ω_4 represents the rigidity of Ln^{3+} chemical environment [24,25]. Their decrease is again in agreement with fluorine richer first coordination shell around Eu^{3+}. Finally, it can be seen that both experimental and radiative lifetimes increase in these samples, suggesting that most PbF_2 concentrated glasses are more suitable hosts for rare earth luminescence. The high quantum efficiency values are also promising results showing the potential of these glasses as luminescent vitreous materials.

4. Conclusion

Glass samples were prepared in the (90-x)TeO_2-10GeO_2-xPbF_2 ternary system with x varying from 5 to 30. These new glass compositions were characterized by DSC, Raman spectroscopy, X-ray diffraction, UV–Vis absorption and Eu^{3+} photoluminescence. PbF_2 incorporation in the tellurite germanate glass network decreases glass transition and thermal stability. Raman spectroscopy allowed to determine structural changes in tellurite units with conversion of TeO_4 to TeO_3 for higher PbF_2 contents whereas UV–Vis investigations pointed out an increase of the optical bandgap related with higher ionic character of the glass network. Photoluminescence measurements revealed that PbF_2 addition promotes important modifications of the Eu^{3+} first coordination shell with a higher symmetry, lower covalence and rigidity of the chemical bonds around europium ions as well as higher experimental lifetimes of the excited state $^5D_0$. All these results are in good agreement with a structural model in which fluorine incorporation progressively breaks the covalent oxide bridging bonds replaced by terminal bonds such as Te—F or Ge—F with a resulting lower connectivity. The europium oxide neighborhood is progressively replaced by fluorine which promotes a higher symmetry and lower local phonon energy. Finally, high quantum efficiency values make these materials interesting candidates for luminescent applications.

Acknowledgments

The authors would like to thank Brazilian funding agencies FAPEMIG (CEX-APQ-01410-12), FINEP (CT-INFRA 2011), CNPq (552225/2011-8) and CAPES for financial support.

References

[1] J.E. Stanworth, Tellurite Glasses, J. Soc. Glas. Technol. 36 (1952) 217–241.
[2] M.A.P. Silva, et al., J. Phys. Chem. Solids 63 (2002) 605–612.
[3] O.L. Malta, L.D. Carlos, Quim. Nova 26 (6) (2003) 889–895.
[4] M.A.P. Silva, et al., J. Phys. Chem. Solids 62 (2001) 1055–1060.
[5] Z. Pan, J. Non-Cryst. Solids 352 (2006) 801–806.
[6] I. Kabalci, et al., J. Alloys Compd. 419 (2006) 294–298.
[7] G. Yankov, L. Dimowa, N. Petrova, M. Tarassov, K. Dimitrov, T. Petrov, B.L. Shivachev, Synthesis, structural and non-linear optical properties of TeO_2–GeO_2–Li_2O glasses, Opt. Mater. 2 (2012) 248–251.
[8] A.G. Kalampounias, N.K. Nasikas, G.N. Papatheodorou, Structural investigations of the xTeO_2-(1-x)GeO_2 (x = 0, 0.2, 0.4, 0.6, 0.8 and 1) tellurite glasses: A composition dependent Raman spectroscopic study, J. Phys. Chem. Solids 9 (2011) 1052–1056.
[9] C. Jiang, P. Deng, J. Zhang, F. Gan, Emission properties of ytterbium-doped GeO_2–TeO_2 glasses, Phys. Lett. A 1 (2004) 91–94.
[10] I. Endo, N. Onouchi, H. Yamaguchi, A. Shimbori, S. Matsumoto, Cathode-luminescence property of Er^{3+}/Yb^{3+}-doped amorphous GeO_2, Opt. Mater. 6–7 (2006) 879–882.
[11] N. Arai, H. Tsuji, M. Hattori, M. Ohsaki, H. Kotaki, T. Ishibashi, Y. Gotoh, J. Ishikawa, Luminescence properties of Ge implanted SiO_2:Ge and GeO_2:Ge films, Appl. Surf. Sci. 4 (2009) 954–957.
[12] V.D. Cacho, L.R.P. Kassab, S.L. Oliveira, R.D. Mansano, P. Verdonck, Blue cooperative luminescence properties in Yb^{3+} doped GeO_2–PbO–Bi_2O_3 vitreous system for the production of thin films, Thin Solid Films 2 (2006) 764–767.
[13] S. Sakida, J. Non-Cryst. Solids 243 (1999) 13–25.
[14] C. Pereira, et al., Thermal and structural study of glasses in the binary system TeO_2-$Pb(PO_3)_2$, J. Non-Cryst. Solids 379 (2013) 180–184.
[15] M.A.P. Silva, et al., Synthesis and structural investigations on TeO_2-PbF_2-CdF_2 glasses and transparent glassceramics, J. Phys. Chem. Solids v 63 (2002) 605–612.
[16] Q.J. Rong, A. Osaka, T. Nanba, J. Takada, Y. Miura, Infrared and Raman of binary tellurite glasses containing boron and indium oxides, J. Mater. Sci. 14 (1992) 3793–3798.
[17] H. Li, Y. Su, S.K. Sundaram, Raman spectroscopic study of Nd-doped $10N_2O$-90TeO_2 glasses, J. Non-Cryst. Solids 1 (2001) 402–409.
[18] T. Komatsu, H. Tawarayama, H. Mohri, K. Matusita, Properties and crystallization behaviors of TeO_2-$LiNbO_3$ glasses, J. Non-Cryst. Solids 2-3 (1991) 105–113.
[19] M. Dimitrova-Pankova, Y. Dimitriev, M. Arnaudov, V. Dimitrov, Infrared spectral investigation of the influence of modifying oxides on the structure of tellurite glasses, Phys. Chem. Glasses 6 (1989) 260–263.
[20] Monteiro, G. et al Local structure around Er^{3+} in GeO_2–TeO_2–Nb_2O_5–K_2O glasses and glass-ceramics. J. Non-Cryst. Solids, v.377, p. 129–136, 2013.
[21] W.A. Pisarski, et al, J. Mol. Struct. 792-793 (2006) 207–211.
[23] Carlos, L. D. et al, Lanthanide-containing light-emitting organic-inorganic hybrids: a bet on the future. Adv. Mater., v.21, n.5, p. 509–534, 2009.
[24] R. Reisfield, C.K. Jorgensen, in: K.A. Gscheidner, L. Eyring (Eds.), Handbook on the Physics and Chemistry of Rare Earth, 1984 North Holland, Amsterdam.
[25] De Sá, G. F et al. Spectroscopic properties and design of highly luminescent lanthanide coordination complexes. Coord. Chem. Rev., v. 196, n1-, pp. 165–195, 2000.